Mechanisms of Stereocontrol for Doubly Silylene-Bridged C_s- and C_1-Symmetric Zirconocene Catalysts for Propylene Polymerization. Synthesis and Molecular Structure of Li$_2$[(1,2-Me$_2$Si)$_2${C$_5$H$_2$-4-(1*R*,2*S*,5*R*-menthyl)}{C$_5$H-3,5-(CHMe$_2$)$_2$)}]·3THF and [(1,2-Me$_2$Si)$_2${η^5-C$_5$H$_2$-4-(1*R*,2*S*,5*R*-menthyl)}{η^5-C$_5$H-3,5-(CHMe$_2$)$_2$}]ZrCl$_2$

Dario Veghini,[†] Lawrence M. Henling,[†] Terry J. Burkhardt,[‡] and John E. Bercaw*,[†]

Contribution from the Arnold and Mabel Beckman Laboratories of Chemical Synthesis, California Institute of Technology, Pasadena, California 91125, and Baytown Polymer Center, Exxon Chemical Company, Baytown, Texas 77520-2101

Abstract: Doubly [SiMe$_2$]-bridged metallocenes (1,2-SiMe$_2$)$_2${η^5-C$_5$H$_2$-4-R}{η^5-C$_5$H-3,5-(CHMe$_2$)$_2$}ZrCl$_2$ (R = H (**1a**), CHMe$_2$ (**1b**), SiMe$_3$ (**1c**), CHMe(CMe$_3$) (**1d**), (+)-menthyl (**1e**)), when activated by methylaluminoxane (MAO), catalyze propylene polymerization with high activities. The preparations and X-ray structures of the dilithio salt of an enantiopure, doubly silylene-bridged bis(cyclopentadienyl) ligand, Li$_2$[(1,2-Me$_2$Si)$_2$-{C$_5$H$_2$-4-(1*R*,2*S*,5*R*-menthyl)}{(C$_5$H-3,5-(CHMe$_2$)$_2$)}]·3THF, as well as the corresponding zirconocene dichloride, [(1,2-Me$_2$Si)$_2${η^5-C$_5$H$_2$-4-(1*R*,2*S*,5*R*-menthyl)}{η^5-C$_5$H-3,5-(CHMe$_2$)$_2$}]ZrCl$_2$ (**1e**), are reported. The C_s-symmetric systems **1a**–**c** are highly regiospecific and syndiospecific (>99.5%) in neat propylene. At lower propylene concentrations, polymers with lower molecular weights and tacticity (mostly *m*-type stereoerrors) are obtained. The microstructures of polymers produced under differing reaction conditions are consistent with stereocontrol dominated by a site epimerization process, an inversion of configuration at zirconium resulting from the polymer chain swinging from one side of the metallocene wedge to the other without monomer insertion. The relative importance of chain epimerization (at the β carbon) has been established by parallel polymerization of 2-d_1-propylene and d_0-propylene with **1b**/MAO at low propylene concentrations. The C_1-symmetric systems **1d,e**/MAO display an unusual dependence of stereospecificity on propylene concentration, switching from isospecific to syndiospecific with increasing propylene pressure, consistent with a competitive unimolecular site epimerization process and a bimolecular chain propagation. The microstructures of the polypropylenes produced by **1d**/MAO and **1e**/MAO with [*r*] ≈ 50% resemble the hemiisotactic microstructure produced by Me$_2$C(η^5-C$_5$H$_3$-3-Me)(η^5-C$_{13}$H$_8$)ZrCl$_2$ (**2b**)/MAO. Contrastingly, the hemiisotactic polypropylene microstructure obtained with **2b**/MAO is found to be maintained at all propylene concentrations examined.

Introduction

Polymerization of α-olefins by metallocene systems is one of the most efficient and selective catalytic reactions, commonly displaying activities and stereoselectivities approaching those of enzymes.[1] Intense efforts have been undertaken to elucidate the mechanistic details of the process in order to correlate polymer properties (tacticity, molecular weight, etc.) with the molecular structure of the catalyst counterpart. C_2-symmetric metallocene catalysts enchain selectively one of the α-olefin enantiofaces to produce highly isotactic polymers. C_1-Symmetric metallocenes may also be isospecific but usually to a lesser extent.[2,4c]

C_s-Symmetric precatalysts such as **1a**–**c** and **2a** enchain α-olefins with regularly alternating enantiofaces and consequently produce syndiotactic polymer.[3,4] Methyl-substituted **2b** generates polypropylene, whose microstructure closely approximates hemiisotactic, one in which every other propylene has been enchained with the same enantioface and the intervening one stereorandomly. Syndiospecificity is believed to arise from three key features: (1) the C_s-symmetric *ansa*-metallocene structure has one cyclopentadienyl possessing bulky substituents flanking the center of the metallocene wedge to direct the

† California Institute of Technology.

‡ Exxon Chemical Co.

(1) Reviews: (a) Brintzinger, H.-H.; Fischer, D.; Mülhaupt, R.; Rieger, B.; Waymouth, R. M. *Angew. Chem., Int. Ed. Engl.* **1995**, *34*, 1143. (b) Horton, A. *Trends Polym. Sci.* **1994**, *2* (5), 158. (c) Bochmann, M. *J. Chem. Soc. Dalton Trans.* **1996**, 255. (d) Fink, G., Mülhaupt R., Brintzinger H. H., Eds. *Ziegler Catalysis, Recent Scientific Innovation and Technological Improvements*; Springer-Verlag: Berlin, 1995.

(2) Giardello, M. A.; Eisen, M. S.; Stern, C. L.; Marks, T. J. *J. Am. Chem. Soc.* **1993**, *115*, 3326.

(3) (a) Herzog, T. A.; Zubris, D. L.; Bercaw, J. E. *J. Am. Chem. Soc.* **1996**, *118*, 11988. (b) Henling, L. M.; Herzog, T. A.; Bercaw, J. E. *Acta Crystallogr.*, submitted. (c) Herzog, T. A. Ph.D. Thesis, California Institute of Technology, 1997. (d) Veghini, D.; Henling, L. M.; Bercaw, J. E. *Inorg. Chim. Acta* **1998**, *280*, 226.
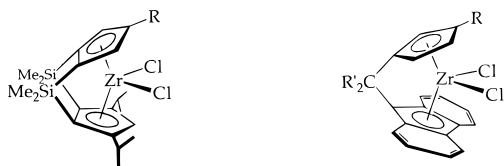
(4) (a) Ewen, J. A.; Jones, R. L.; Razavi, A.; Ferrara, J. D. *J. Am. Chem. Soc.* **1988**, *110*, 6255. (b) Ewen, J. A.; Elder, M. J.; Jones, R. L.; Curtis, S.; Cheng, H. N. *Stud. Surf. Sci. Catal.* **1990**, *56*, 439. (c) Ewen, J. A.; Elder, M. J.; Jones, L.; Haspeslagh, L.; Atwood, J. L.; Bott, S. G.; Robinson, K. *Makromol. Chem., Makromol. Symp.* **1991**, *48/49*, 253. (d) Ewen, J. A.; Elder, M. J. *Makromol. Chem. Makromol Symp.* **1993**, 66. (e) Ewen, J. A.; Elder, M. J. Eur. Pat. Appl. EP-A 0 537 130, 1993. (f) Ewen, J. A. *Makromol. Chem., Makromol. Symp.* **1995**, 181.

1	R = H (**1a**)
	R = CHMe$_2$ (**1b**)
	R = SiMe$_3$ (**1c**)
	R = *rac*-CH(Me)(CMe$_3$) (**1d**)
	R = (1*R*, 2*S*, 5*R*)-menthyl (**1e**)

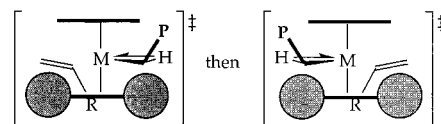| 2 | R = H; R' = Me (**2a**) |
| | R = R' = Me (**2b**) |
| 3 | R = H; R' = Ph |

polymer chain segment (up) toward the less substituted cyclo-pentadienyl, whether it resides on the left or right side in the transition structure for propagation (Scheme 1); (2) an open region between the bulky substituents on the lower cyclopen-tadienyl to accommodate the α-olefin alkyl (methyl for propy-lene), which is directed by the polymer segment trans (down), the dominant steric interaction in the transition structure;[5,6] and (3) migratory insertions that result in regular alternation of the monomer approach from the left and right side of the metal-locene wedge.

Our laboratory recently reported the preparation of C_s- and C_1-symmetric catalysts **1a**−**d** along with some preliminary data on their polymerization behavior.[3a] The C_s-symmetric precata-lysts **1a**−**c**, when activated with methylaluminoxane, display high activity and syndioselectivity and produce high-molecular-weight polymers. On the other hand, C_1-symmetric systems display a remarkable dependence of stereospecificity with increasing propylene concentration, switching from isospecific to syndiospecific. In this contribution, we report the results of some recent investigations on the mechanisms of stereocontrol operating in these catalytic systems.
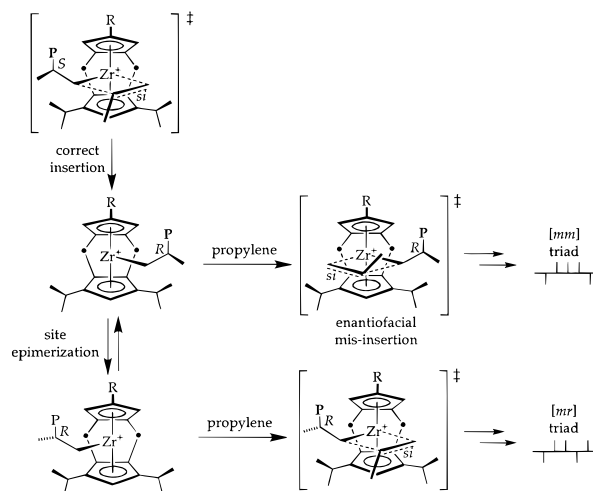
Results and Discussion

Dependence of Stereoselectivity on Monomer Concentra-tion in C_s-Symmetric 1a−c/MAO. Although the stereospeci-ficities of catalysts derived from **1a**−**c** and **2a** are high at low temperatures in liquid propylene, under other conditions pro-pylene enchainment does not occur with perfectly alternating olefin enantiofaces, and isolated *m* or *mm* stereoerrors are produced. Three types of stereoerror mechanisms are generally considered for these C_s-symmetric systems (Schemes 2 and 3): (1) enantiofacial misinsertion, giving an [*mm*] triad, the number of which is independent of the concentration of propylene (Scheme 2); (2) site epimerization (chain migration without insertion), giving an isolated *m* stereoerror (Scheme 2); and (3) chain epimerization,[7−9] giving either *m* or *mm* stereoerrors, depending on the whether stereochemistry at the metal center is inverted or retained (Scheme 3). Since the epimerization processes are unimolecular and compete with bimolecular
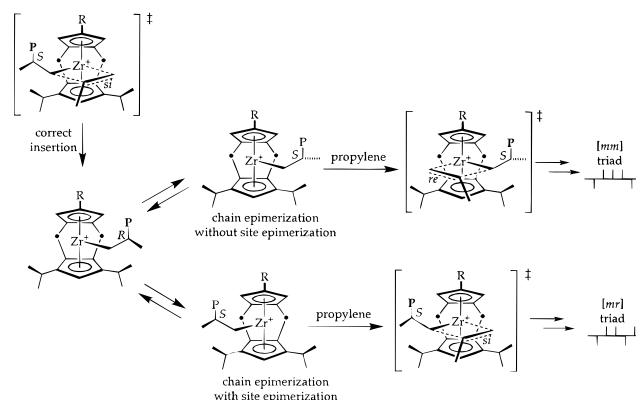
(5) (a) Corradini, P.; Guerra, G.; Vacatello, M.; Villani, V. *Gazz. Chim. Ital.* **1988**, *118*, 173. (b) Corradini, P.; Guerra, G.; Cavallo, L.; Moscardi, G.; Vacatello, M. Ziegler Catalysis. In *Ziegler Catalysis, Recent Scientific Innovation and Technological Improvements*; Fink, G., Mülhaupt R., Brintzinger H. H., Eds.; Springer-Verlag: Berlin, 1995; p 237. (c) Guerra, G.; Corradini, P.; Cavallo, L.; Vacatello, M. *Makromol. Chem., Makromol. Symp.* **1995**, *89*, 77.

(6) Gilchrist, J. H.; Bercaw, J. E. *J. Am. Chem. Soc.* **1996**, *118*, 12021.

(7) (a) Busico, V.; Cipullo, R. *J. Am. Chem. Soc.* **1994**, *116*, 9329. (b) Busico, V.; Caporaso, L.; Cipullo, R.; Landriani, L. *J. Am. Chem. Soc.* **1996**, *118*, 2105. (c) Busico, V.; Brita, D.; Caporaso, L.; Cipullo, R.; Vacatello, M. *Macromolecules* **1997**, *30*, 3971.

(8) Resconi, L.; Fait, A.; Piemontesi, F.; Colonnesi, M.; Rychlicki, H.; Ziegler, R. *Macromolecules* **1995**, *28*, 6667.

(9) Leclerc, M. K.; Brintzinger, H.-H. *J. Am. Chem. Soc.* **1995**, *117*, 1651; **1996**, *118*, 9024.

Scheme 1

Scheme 2

Scheme 3

propagation, the frequency of stereoerrors produced by processes 2 and 3 should depend on propylene concentration.

There are some curious differences in the behavior of the singly linked fluorenyl/cyclopentadienyl catalyst system **2**. The numbers of isolated *m* stereoerrors and [*mm*] triads produced by catalyst **2a**/MAO have been reported to increase with decreasing propylene concentration. Some residual [*mm*] triads were observed at all propylene concentrations examined.[4] By contrast, the stereoselectivity displayed by C_1-symmetric **2b**/MAO was found to be relatively constant under all conditions studied,[10] and the observed polymer microstructure, closely resembling hemiisotactic, was rationalized by invoking a regular alternation of stereospecific olefin insertion (with propylene adding to the more hindered side of the metallocene wedge), followed by aspecific insertion (with propylene adding to the less hindered side).[11,12] Competitive site epimerization and chain propagation were invoked in the other cases.[13] Thus, the relative rates of propagation vs site epimerization for catalyst systems

(10) Herfert, N.; Fink, G. *Makromol. Chem., Makromol. Symp.* **1993**, *66*, 157.

(11) Farina, M.; DiSilvestro, G.; Sozzani, P. *Macromolecules* **1993**, *26*, 946.

(12) Cavallo, L.; Guerra, G.; Vacatello, M.; Corradini, P. *Macromolecules* **1991**, *24*, 1784.

Table 1. Propylene Polymerization Data with **1a−c**/MAO at 24 ± 1 °C in Toluene Solution (Entry Numbers Are Correspondingly the Same as for Table 2)

entry	catalyst	$[C_3H_6]$ (M)	activity[a]	$[r]$ (%)	T_m (°C)	M_w	M_w/M_n
1	**1a**	0.8	3×10^3 [b]	90.6	109	2.9×10^4	1.9
2	**1a**	1.5	1.3×10^4 [b]	95.0	nd[c]	nd	nd
3	**1a**	2.1	2.9×10^4 [b]	94.7	131	6.1×10^4	3.0
4	**1a**	2.8	3.1×10^4 [b]	95.9	139	9.0×10^4	4.2
5	**1a**	3.4	5.3×10^4 [b]	97.1	140	1.01×10^5	1.5
6	**1b**	0.8	1.9×10^4	80.2	nd	3.4×10^4	2.5
7	**1b**	1.5	1.9×10^4	91.8	d	5.9×10^4	2.4
8	**1b**	2.1	3.5×10^4	92.7	d	1.46×10^5	1.7
9	**1b**	2.9	5.9×10^4	95.1	118	1.15×10^5	3.0
10	**1b**	3.4	1.04×10^5	97.1	127	1.66×10^5	1.8
11	**1c**	0.8	7×10^3	81.5	d	3.8×10^4	1.9
12	**1c**	1.5	2.4×10^4	86.7	d	4.9×10^4	2.2
13	**1c**	2.1	4.3×10^4	90.7	102	7.7×10^4	1.7
14	**1c**	2.8	5.4×10^4	93.6	119	nd	nd
15	**1c**	3.4	5.7×10^4	96.5	124	1.33×10^5	1.8

[a] Defined as grams of polymer per gram of Zr per hour. [b] A different sample of methylalumoxane cocatalyst was employed for entries 1−5. The activity data are therefore not comparable with entries 6−15. [c] Not determined. [d] No melting point observed by DSC.

2a/MAO and **2b**/MAO appear to depend explicitly on the nature of the substituent R.

To quantify the relative contributions of [propylene]-dependent and [propylene]-independent stereoerrors for catalyst systems **1a−c**/MAO, polymerizations were carried out at 24 ± 1 °C in toluene solution at various propylene pressures to effect a propylene concentration range 0.8−3.4 M. The reproducibilities of the polymer yield and molecular weight, as well as the influence of [MAO]/[Zr] ratio on activity and polymer tacticity, were investigated. Polymerization reactions carried out under the conditions described gave reproducible r diad contents ($\{^1H\}^{13}C$ NMR) with composite errors amounting to approximately ±2%. The [MAO]/[Zr] ratio significantly influences the catalyst activity, but the polymer tacticity is unaffected, at least over the range examined.[14] No regioerrors ("2,1" or "3,1" errors) with any of the catalysts under any conditions investigated were detected by ^{13}C NMR spectroscopy, as was reported earlier for catalyst **2a**.[3a,4]

The variations of $[r]$ diad contents with varying propylene concentration are given in Table 1 and Figure 1. The stereoselectivities for all three catalysts **1a−c**/MAO are comparable at [propylene] > 3.5 M but differ significantly at lower concentrations. As the [propylene] increases, the $[r]$ diad content rises moderately for **1a** and more significantly for **1b** and **1c**. The mm and (substantially more) m stereoerrors follow a similar trend (Figure 2), decreasing with increasing [propylene] over the entire range of concentrations examined. At low propylene concentrations, 2−3% mm stereoerrors are detected for all catalysts, while at higher concentration these are no longer detectable for **1b** and **1c**, accounting for less than 1% for **1a**.

Thus, stereoselectivity increases with propylene concentration, indicating that enantiofacial misinsertion is not the major

(13) (a) Rieger, B.; Jany, G.; Fawzi, R.; Steimann, M. *Organometallics* **1994**, *13*, 647. (b) Gauthier, W. J.; Collins, S. *Macromolecules* **1995**, *28*, 3779. (c) Jany, G.; Repo, T.; Gustafsson, M.; Leskelä, M.; Polamo, M.; Kliga, M.; Dietrich, U.; Rieger, B. *Chem. Ber./Recl.* **1997**, *130*, 747. (d) Waymouth, R. Oral presentation at the Meeting "Advances in Polyolefin", Napa Valley, CA, 1997. (e) For a related example in a heterogeneous system, see: Busico, V.; Cipullo, R.; Talarico, G.; Segre, A. L.; Chadwick, J. C. *Macromolecules* **1997**, *30*, 4786.

(14) [MAO]/[Zr] ratios in the range from 50:1 to 15 000:1 were investigated. The activity reaches a maximum about 7000:1, but the $[r]$ content is found to be essentially independent (±3%) of the Al/Zr molar ratio.

stereoerror mechanism. The strong dependence of the isolated m stereoerrors with [propylene] further suggests that site epimerization and olefin insertion occur at competitive rates over this range of monomer concentrations, tentatively permitting us to assign the major stereoerror-producing process to site epimerization (Scheme 2). The remaining errors would then be attributable to a less frequent chain epimerization, giving rise to a few percent mm-type, and becoming apparent only at the lowest propylene concentrations. Nonetheless, these results do not allow us to exclude another possibility: that the isolated m stereoerrors arise from the combination of chain epimerization and site epimerization (Scheme 3), i.e., that chain epimerization occurs mostly with simultaneous site epimerization (giving an isolated m) and only occasionally without site epimerization (giving rise to an mm stereoerror).

We therefore further examined the importance of chain epimerization by performing a labeling study analogous to the those described by Brintzinger and Busico.[7,9] The number of stereoerrors (isolated m and mm types, Scheme 3) that arise from chain epimerization should decrease in proportion to the kinetic deuterium isotope effect for β-H elimination, $(k_1)^L$ (L = H, D) or, alternatively, in proportion to the preequilibrium deuterium isotope effect for β-H elimination, $(K_1)^L$ (Scheme 4). Parallel polymerization reactions using d_0-propylene and 2-d_1-propylene as a substrates were thus carried out, and the microstructures of the poly-d_0-propylene and poly-2-d_1-propylenes so obtained were compared.

The good precatalyst candidate for the experiments comparing unlabeled and deuterium-labeled propylenes appeared to be **1b**, since at [propylene] = 0.8 M it produces a large number of mm and isolated m stereoerrors. The reactions were performed in toluene solution saturated with propylene (1 atm, [propylene] = 0.8 M) at room temperature. As can be seen from the results presented in Table 3, although the molecular weights differ, the poly-2-d_1-propylene and poly-d_0-propylene samples so obtained have essentially the same microstructures within experimental error ($\{^1H\}^{13}C$ NMR). The number-average molecular weight of poly-d_0-propylene (32 800) vs poly-2-d_1-propylene (56 800) implies a kinetic deuterium isotope effect for chain transfer $k(\beta$-H$)/k(\beta$-D$) = 1.6$, assuming β-H transfer as the predominant chain transfer pathway.

The $\{^1H\}^2H$ NMR spectrum of poly-2-d_1-propylene displays two broad signals at 1.4 and 0.5 ppm in an approximately 50:1 ratio.[15] We tentatively assign the former to $-CD(CH_3)-$ groups and the latter to ca. 2% $-CH(CH_2D)-$ groups arising from chain epimerization (Scheme 4). This assignment is in agreement with the finding of 2−3% mm stereoerrors for **1b**/MAO under similar conditions, implicating chain epimerization as the major source of the mm stereoerrors. More importantly, the observation that poly-2-d_1-propylene has essentially the same microstructure (in fact, slightly more (19.6% vs 17.3%), not fewer $[rmrr]$ pentads, as would be expected from a normal deuterium isotope effect for β-H elimination), together with the observed dependence of stereospecificity on propylene concentration, allows us to confidently assign site epimerization as the principal process for stereoerror formation with the catalyst system **1a−c**/MAO.

Temperature Effects on the Polymerization Behavior of 1a−c/MAO Catalyst Systems. A significant temperature influence on stereoselectivity is expected for syndiospecific catalyst systems **1a−c**/MAO, where a first-order stereoerror process (site

(15) The $\{^1H\}^2H$ NMR spectra were recorded at 80 °C in $C_6H_3Cl_3/C_6H_6$ solution containing a small amount of benzene-d_6, externally lock-shimmed in the ^1H channel on a separate $C_6H_3Cl_3/C_6D_6$ sample having no polymer. The ^2H chemical shifts (100 transients) are referenced to the small amount of benzene−d_6.

Table 2. Pentad Distributions (%) for the Polypropylene Samples Produced by **1a**−**c**/MAO at 24 ± 1 °C in Toluene Solution (Entry Numbers Are Correspondingly the Same as for Table 1)

entry	catalyst	[mmmm]	[mmmr]	[rmmr]	[mmrr]	[mrmm]+ [rmrr]	[mrmr]	[rrrr]	[mrrr]	[mrrm]
1	**1a**			1.7	3.6	11.6		68.6	14.4	
2	**1a**		<1		1.5	5.1		79.5	13.5	
3	**1a**		<1		2.1	4.7		83.6	9.0	
4	**1a**		<1		2.0	3.5		86.1	7.7	
5	**1a**		<1		1.9	2.7		90.7	4.2	
6	**1b**		1.4	3.0	6.0	19.9	5.1	41.5	20.4	2.5
7	**1b**				2.3	12.6	<1	68.2	17.0	
8	**1b**			<1	1.4	10.3	<1	71.6	13.3	2.6
9	**1b**				1.3	8.6		82.6	7.4	
10	**1b**					5.5		89.0	5.5	
11	**1c**	<1	1.2	2.4	5.3	18.8	4.2	47.2	18.0	1.7
12	**1c**			1.7	3.6	16.7	3.4	59.0	15.0	
13	**1c**		<1		2.1	13.0	1.3	68.9	13.5	
14	**1c**				2.4	7.8		75.8	12.7	1.2
15	**1c**					7		81.6	11.3	
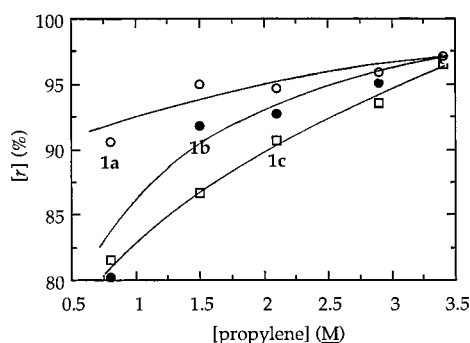
Figure 1. Dependence of [r] diads on propylene concentration for C_s-symmetric catalysts **1a**−**c**/MAO.
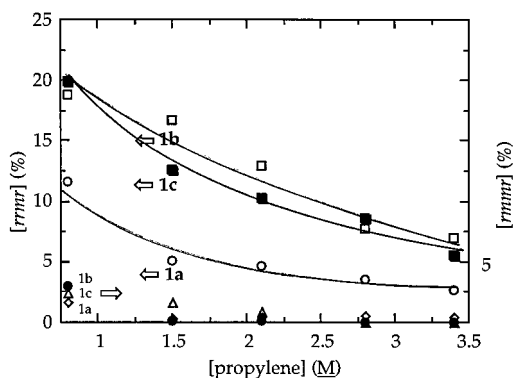
Figure 2. Dependence of [rmrr] and [rmmr] pentads on propylene concentration for C_s-symmetric catalysts **1a**−**c**/MAO.

Scheme 4
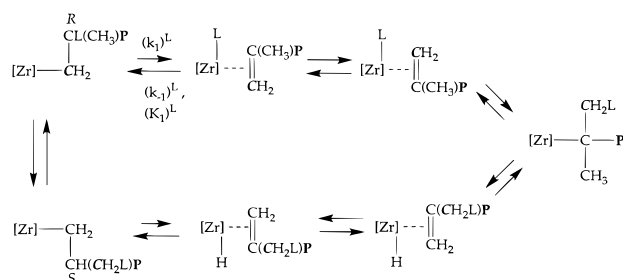
([Zr] = Cp$_2$Zr$^+$; L = H, D; **P** = remaining polymer chain)

epimerization) competes with a second-order chain propagation process. Under conditions where a first-order process and a second-order process have comparable rates, and hence comparable activation free energies, the second-order process is

Table 3. Polymer Analyses for Poly-d_0-propylene and Poly-2-d_1-propylene Produced by **1b**/MAO in Toluene Solution at 1 atm Propylene, 25 °C

polymer	[r] (%)	[rmrr] ([mrmm]+) (%)	[rmmr] (%)	M_n	M_w/M_n
poly-d_0-propylene	83.3	17.3	2.2	32 840	1.9
poly-2-d_1-propylene	84.2	19.6	1.6	56 830	1.8

Table 4. Propylene Polymerization Data with **1a**−**e** and (Ph$_2$C)[(η^5-C$_5$H$_4$)(η^5-C$_{13}$H$_8$)]ZrCl$_2$ (**3**)/MAO in Liquid Propylene (Entry Numbers Are Correspondingly the Same as for Table 5)

entry	catalyst	T (°C)	activity[a]	[r] (%)	T_m (°C)	M_w	M_w/M_n
16	**1a**	20	2.8×10^6	97.1	151	1.25×10^6	1.9
17	**1a**	50	7.9×10^6	96.6	140	3.3×10^5	2.3
18	**1a**	70	16.9×10^6	94.1	119	1.6×10^5	3.2
19	**1b**	20	3.2×10^5	99.4	151	9.8×10^5	2.0
20	**1b**	50	1.4×10^6	94.5	123	2.9×10^5	2.0
21	**1b**	70	9.2×10^5	90.6	b	1.3×10^5	2.3
22	**1c**	20	3.5×10^5	97.9	152	7.9×10^5	1.8
23	**1c**	50	8.3×10^5	96.0	124	2.6×10^5	2.1
24	**1c**	70	7.3×10^5	91.3	b	1.4×10^5	2.2
25	**1d**	20	2.5×10^5	75.4	102	1.9×10^5	2.2
26	**1e**	20	4.9×10^5	78.7	b	4.7×10^5	1.9
27	**3**	20	1.3×10^5	99.2	147	8.4×10^5	2.3
28[c]	**3**	40	$2.0 \times 10^{4 c}$	95.6	137	3.8×10^5	2.0
29[c]	**3**	60	$9.0 \times 10^{4 c}$	94.4	132	2.7×10^5	2.0

[a] Defined as grams of polymer per gram of Zr per hour. [b] No melting point observed by DSC. [c] These two runs were carried out earlier with a differing catalyst:MAO ratio (1:325) and with propylene of generally lower purity that for the other runs.

typically characterized by a much more negative $\Delta S^\ddagger$ and commensurably smaller $\Delta H^\ddagger$ as compared with the first-order process. Thus, we expect that site epimerization (larger $\Delta H^\ddagger$) would become more important (relative to propagation with smaller $\Delta H^\ddagger$) at higher temperatures, and a strong temperature dependence of stereospecificity would obtain.

To establish the influence of temperature on activity and stereospecificity for catalysts **1a**−**c**/MAO, polymerization reactions were performed in neat propylene at 20, 50, and 70 °C (Tables 4 and 5). A singly bridged cyclopentadienyl/fluorenyl catalyst system,[16] Ph$_2$C(η^5-C$_5$H$_4$)(η^5-C$_{13}$H$_8$)ZrCl$_2$ (**3**)/MAO,[16b] was also examined for comparison. Catalyst **1a** is the most active system of the series, producing about 1.6×10^7 g of polymer g of polymer g^{-1} Zr h^{-1}, as compared with less than 1×10^6 g of polymer g^{-1} Zr h^{-1} for the others at 70 °C. Moreover,

(16) (a) Razavi, A.; Atwood, J. L. *J. Organomet. Chem.* **1993**, *459*, 117. (b) Winter, J.; Rohrmann, M.; Dolle, V.; Spaleck, W. Eur. Pat. Appls. 0,-387,690 and 0.387,691, 1991.

Table 5. Pentad Distribution (%) for the Polypropylene Produced by **1a**−**e** and (Ph$_2$C)[(η^5-C$_5$H$_4$)(η^5-C$_{13}$H$_8$)]ZrCl$_2$ (**3**)/MAO in Liquid Propylene (Entry Numbers Are Correspondingly the Same as for Table 4)

entry	catalyst	[*mmmm*]	[*mmmr*]	[*rmmr*]	[*mmrr*]	[*mrmm*] + [*rmrr*]	[*mrmr*]	[*rrrr*]	[*mrrr*]	[*mrrm*]
16	**1a**			0.8	1.5	0.9		93.4	3.5	
17	**1a**			<1	2.0	2.4		90.6	4.9	
18	**1a**			<1	3.0	7.3	<1	79.5	10.0	
19	**1b**			-	-	1.2		97.5	1.2	
20	**1b**			1.6	1.9	4.2		81.0	11.1	
21	**1b**			1.8	2.4	12.9	<1	68.4	14.3	
22	**1c**			0.3	0.6	1.6		94.2	3.3	
23	**1c**			-	1.2	4.8		83.8	10.1	
24	**1c**			<1	3	13.6	<1	65.8	17.1	
25	**1d**	1.3	4.4	4.0	14.4	6.6		49.5	17.5	2.3
26	**1e**	3.3	4.5	6.0	12.9	11.4		45.4	13.7	2.8
27	**3**				1.2			97.5	1.2	
28[a]	**3**			1.5	3.1	2.0	0.8	83.6	9.1	
29[a]	**3**		0.5	1.7	3.4	2.6	0.9	81.1	9.3	0.6

[a] These two runs were carried out earlier with a differing catalyst:MAO ratio (1:325) and with propylene of generally lower purity than that for the other runs.

while the activities for **1b** and **1c** decrease on going from 50 to 70 °C (probably due to partial catalyst decomposition at elevated temperatures), **1a** reaches its maximum at 70 °C. No regioerrors are detected at any of the temperatures examined.

Stereocontrol is generally high at 20 °C ([*r*] = >99%), but a moderate decrease in tacticity at higher temperatures for **1a** is more pronounced for **1b** and **1c**. In all cases, at *T* = 70 °C, isolated [*m*] diads constitute the main type of stereoerrors present in the polymer microstructure ([*rmrr*] = 7−12% for all catalysts), while [*rmmr*] pentads account for less than 3% of the stereoerrors. At 20 °C, the stereocontrol displayed by **1b** is comparable to that found for **3**, slightly better than those for **1a** and **1c**. Assuming an equal number of active sites for all catalysts, a considerably higher rate of propagation for **1a** is also indicated.

The polymerization experiments in neat propylene at 20 °C with **1a**−**c**/MAO and **3**/MAO produced syndiotactic polymers with high melting points (T_m > 150 °C for **1a**−**c**/MAO, T_m = 147 °C for **3**/MAO). The molecular weights are in the order of 1 000 000 decreasing to about 100 000 at 70 °C (PDIs = 1.8−3.2).
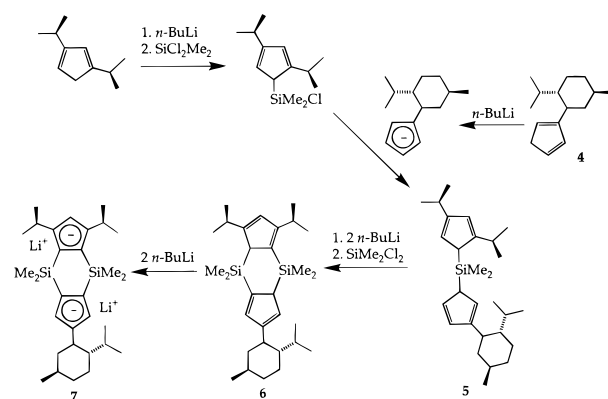
C_1-Symmetric Systems. In a preliminary report,[3a] we noted the exceptional behavior of C_1-symmetric **1d**, which appeared to switch from isospecific to syndiospecific with increasing propylene concentrations.[17] Another C_1-symmetric system was therefore prepared to examine the scope of this "ambispecificity" for systems bearing a chiral substituent at the central position of the (upper) cyclopentadienyl ligand. Enantiopure (+)-menthyl was chosen for the preparation of doubly [SiMe$_2$]-bridged zirconocene dichloride **1e**. Although we anticipated no difference in the performance of a catalyst having an enantiopure substitutent rather than a racemic one, the availability of the precursor to **1e** only in enantiopure form led us to incorporate (+)-menthyl.

(1*R*,2*S*,5*R*)-Menthylcyclopentadiene was prepared according to a procedure closely analogous to that reported by Marks and co-workers.[18] The steps shown in Scheme 5 proceeded in high yields, giving **6** as a high-boiling oil.[19] The dilithio salt Li$_2$[(1,2-Me$_2$Si)$_2$\{η^5-C$_5$H$_2$-4-(1*R*,2*S*,5*R*-menthyl)\}\{η^5-C$_5$H-3,5-(CHMe$_2$)$_2$\}]·3THF (**7**) was crystallized from THF/petroleum ether, and its

Scheme 5

structure[20] was determined by an X-ray diffraction study[21] (Figure 3). The very soluble dilithio salt **7** may be metalated successfully using ZrCl$_4$ in situ (see Experimental Section), affording **1e** (eq 1). The ^{1}H NMR spectral data and the X-ray crystal structure data for **1e**[22] (Figure 4) confirmed the molecular geometry shown in eq 1.

(1)

Dependence of Stereoselectivity on Monomer Concentration with the 1d,e/MAO Catalyst Systems. Polymerization reactions were performed in toluene solution in the propylene
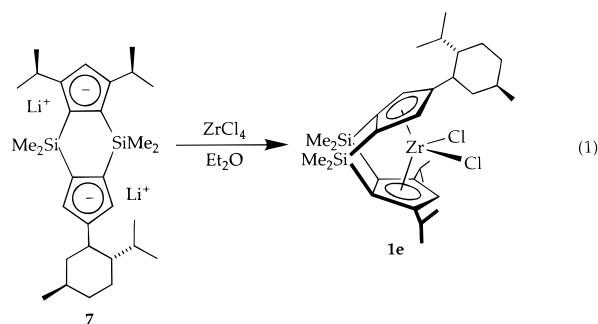
(17) For a catalyst system that switches from moderately isospecific to moderately syndiospecific as a function of temperature, see: Erker, G.; Fritze C. *Angew. Chem., Int. Ed. Engl.* **1992**, *31*, 199.

(18) (a) Giardello, M. A.; Conticello, V. P.; Brard, L.; Sabat, M.; Rheingold, A. L.; Stern, C. L.; Marks, T. J. *J. Am. Chem. Soc.* **1994**, *116*, 10212. (b) Gagné, M. R.; Brard, L.; Conticello, V. D.; Giardello, M. A.; Stern, C.; Marks, T. J. *Organometallics* **1992**, *11*, 2003.

(19) Because of the rapid fluxionality of neutral, silyl-substituted cyclopentadienyl compounds **5** and **7**, the NMR spectra are complex and thus are not diagnostic (see Jutzi, P. *Chem. Rev.* **1988**, *86*, 983). More informative NMR analyses could be performed on the lithium salts of these derivatives.

(20) (a) Hiemeier, J.; Köhler, F. H.; Müller, G. *Organometallics* **1991**, *10*, 11787. (b) Siemeling, U.; Jutzi, P.; Neuman, B.; Stammler, H.-G. *Organometallics* **1992**, *11*, 1328.
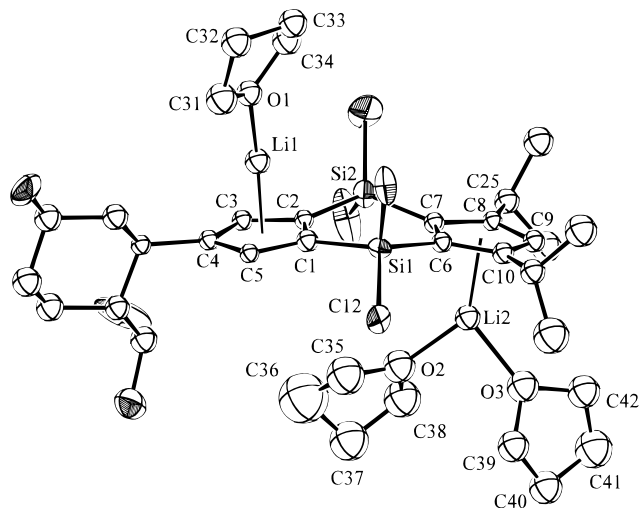
Doubly Silylene-Bridged Zirconocene Catalysts

J. Am. Chem. Soc., Vol. 121, No. 3, 1999 **569**

Figure 3. Molecular structure of [Li]$_2$[(Me$_2$Si)$_2$(η^5-C$_5$H$_2$-4-(1R,2S,5R-menthyl)(η^5-C$_5$H-3,5-(CHMe$_2$)$_2$)]·3THF (**8**). One of the molecules contained in the asymmetric unit is shown (molecule A), the other being essentially isostructural. Hydrogen atoms and some carbon atom labeling is omitted for clarity.

Figure 4. Molecular structure of (Me$_2$Si)$_2$[η^5-C$_5$H$_2$-4-(1R,2S,5R-menthyl)] [η^5-C$_5$H-3,5-(CHMe$_2$)$_2$]ZrCl$_2$ (**1e**). Hydrogen atoms and carbon atom labeling are omitted for clarity.

concentration range 0.5−4.6 M at 25 °C. The results are given in Tables 6 and 7. As can be seen in Figure 5, there is a nearly linear increase of [r] diad content with increasing propylene concentration over this range for both **1d** and **1e**, the former displaying a slightly stronger response than the latter. Contrastingly, the tacticity for polypropylene prepared with the **2b**/MAO catalyst system remains essentially constant over the entire concentration range.[23] The comparatively large changes in the pentad distribution for **1d** are further illustrated in Figure 6. For **1e**, the limit in syndiospecificity at [propylene] = 4.6 M is close to what is observed in neat propylene at 25 °C ([r] = 74.5% vs [r] = 78.7%, respectively). At 0 °C in neat propylene,

Table 6. Propylene Polymerization Data with **1d**,**e**/MAO in Toluene Solution (Entry Numbers Are Correspondingly the Same as for Table 7)

entry	catalyst	[C$_3$H$_6$] (M)	activity[a]	[r] (%)	T_m (°C)	M_w	M_w/M_n
28	**1d**	0.5	2.0×10^3	11.5	nd[b]	nd	nd
29	**1d**	0.8	2.0×10^3	11.3	108	1.9×10^4	1.8
30	**1d**	2.1	2.5×10^3	38.6	b	3.5×10^4	2.0
31	**1d**	3.4	5.3×10^3	53.7	b	nd	b
32	**1d**	4.6	1.0×10^4	63.3	c	4.8×10^4	2.8
33	**1e**	0.5	2.0×10^3	40.3	b	nd	b
34	**1e**	0.8	4.0×10^3	44.2	80	4.0×10^4	1.9
35	**1e**	2.1	8.5×10^3	54.6	106	6.2×10^4	1.6
36	**1e**	3.4	1.8×10^4	67.7	b	nd	b
37	**1e**	4.6	2.5×10^4	74.5	c	1.5×10^5	1.6

[a] Defined as grams of polymer per gram of Zr per hour. [b] Not determined. [c] No melting point observed by DSC.

(21) Suitable crystals for X-ray structure analysis of **7** were obtained from a petroleum ether/Et$_2$O solution containing a few drops of THF. Crystallographic data: a = 9.919(7) Å, b = 15.117(9) Å, c = 15.554(9) Å, α = 75.15(5)°, β = 85.85(5)°, γ = 74.81(5)°; V = 2176(2) Å^3; Z = 2; space group $P\bar{1}$. Data (11 635 reflections, θ_{max} = 22.5°, GOF$_{merge}$ = 1.00) were collected on a CAD-4 diffractometer with Mo Kα (λ = 0.7107) at 160 K. Final solution parameters: R = 0.078 for 3057 reflections with F_o^2 > 3σ(F_o^2); GOF = 1.50 for 480 parameters and 5668 reflections; largest excursions in final difference map were 0.76 e Å^{-3}, −0.79 e Å^{-3}. The two molecules in the asymmetric unit are related by an approximate center of symmetry and have similar conformations and geometric parameters. There is slight disorder in a few of the THF ligands. The most relevant bonds (averages) are given here: Li1−C$_{Cp}$ = 2.17 Å, Li2−C$_{Cp}$ = 2.29 Å, Li1−Cp$_{centroid}$ = 1.80 Å, Li2−Cp$_{centroid}$ = 1.94 Å, Li1−O1 = 1.88 Å, Li2−O = 2.02 Å, Cp$_{centroid}$−Li1−O1 = 168°.

(22) The crystals used for the X-ray structure analysis of **1e** were obtained from a concentrated petroleum ether/(SiMe$_3$)$_2$O solution. Crystallographic data: a = 12.094(6) Å, b = 15.285(9) Å, c = 25.949(17) Å, α = 90.52-(5)°, β = 98.47(5)°, γ = 90.28(4)°; V = 4744(5) Å^3; Z = 6; space group $P\bar{1}$. Data (22 659 reflections, θ_{max} = 22.5°, GOF$_{merge}$ = 1.20) were collected on a CAD-4 diffractometer with Mo Kα (λ = 0.7107) at 160 K. The crystal was non-merohedrally twinned by rotation of 180° about the b-axis. As a result, all non-hydrogen atoms were refined isotropically, and several groups of atoms were restrained to have similar geometries for all six molecules. The six molecules are related pairwise by a pseudocenter; the three pairs by approximate translations along [1 −1 1]. Final solution parameters: R = 0.115 for 9453 reflections with F_o^2 > 2σ(F_o^2); GOF = 2.96 for 692 parameters, 693 restraints, and 20 826 reflections; largest excursions in final difference map were 9.1 e Å^{-3}, −4.8 e Å^{-3}. Relevant bond distances and angles (average): Zr−Cp1 = 2.22 Å, Zr−Cp2 = 2.24 Å, Zr−Cl = 2.43 Å, Cp1−Zr−Cp2 = 122°, Cl−Zr−Cl = 105°. Both **1e** and **1b** (ref 3b,c) have similar conformations.

(23) The pentad distributions (average, %) for polypropenes produced by **2b** in the propene concentration range 0.8−4.6 M with [r] = 55.3 and 49.2, respectively, are [$mmmm$] = 14, [$mmmr$] = 12, [$rmmr$] = 6, [$mmrr$] = 25, [$rmrr$] + [$mrmm$] = 2, [$rmrm$] absent, [$rrrr$] = 21, [$mrrr$] = 14, [$mrrm$] = 5. The polymer microstructure is essentially identical at 0 °C in neat propene.

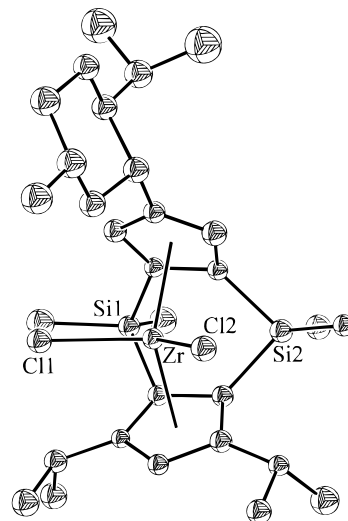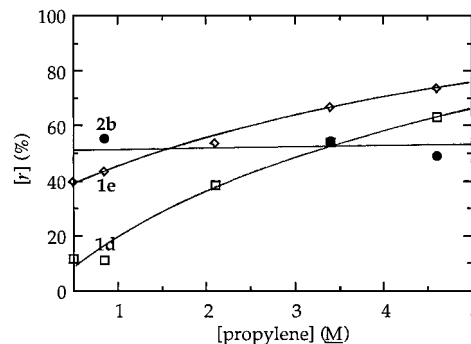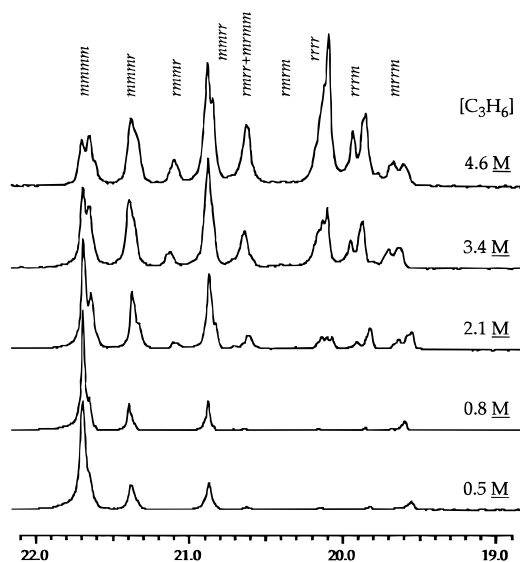**Figure 5.** Dependence of the [r] diads on propylene concentration for C_1-symmetric catalysts **1d**,**e** and **2b**.

the stereocontrol improves considerably ([r] = 90.4%), as expected with a polymerization system where a unimolecular site epimerization process occurs in competition with a bimolecular chain propagation (vide supra). At [propylene] = 0.5 M, the pentad relationship of [$mmmr$]:[$mmrr$]:[$mrrm$] ≈ 2:2:1 displayed by **1d**/MAO is characteristic of isospecific catalysts operating under enantiomorphic site control.
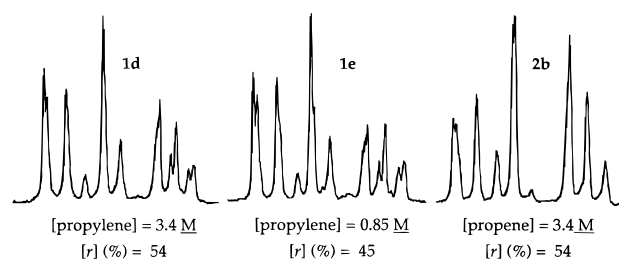
Assuming that, as for **1a**−**c**/MAO, site epimerization also competes with propagation for propylene polymerizations with catalysts **1d**/MAO and **1e**/MAO, we can rationalize the observed polymerization behavior for the latter two systems as follows: at higher propylene concentrations, migratory insertions occur

Table 7. Pentad Distribution (%) for the Polypropylene Produced by **1d**,**e**/MAO in Toluene Solution (Entry Numbers Are Correspondingly the Same as for Table 6)

entry	catalyst	[*mmmm*]	[*mmmr*]	[*rmmr*]	[*mmrr*]	[*mrmm*] + [*rmrr*]	[*mrmr*]	[*rrrr*]	[*mrrr*]	[*mrrm*]
28	**1d**	65.6	14.4	<1	13.6	<1	<1	<1	<1	3.8
29	**1d**	65.5	13.0	<1	12.8	<1	<1	<1	<1	4.2
30	**1d**	29.3	16.6	3.2	18.1	7.3	<1	7.2	8.8	9.1
31	**1d**	17.7	15.0	3.3	19.9	9.1		14.6	12.0	8.3
32	**1d**	9.9	11.6	3.7	18.9	10.3		23.9	16.2	5.7
33	**1e**	26.3	15.3	3.8	17.2	8.9	3.0	7.0	8.5	9.7
34	**1e**	18.6	15.9	2.6	21.5	9.4	<1	11.2	11.8	8.2
35	**1e**	11.5	12.9	4.4	19.5	12.1		18.8	13.3	7.4
36	**1e**	4.3	8.1	3.9	14.7	11.4		34.4	17.2	5.9
37	**1e**	1.6	6.8	2.6	16.1	11.4		38.3	19.3	3.8

Figure 6. Methyl region of the $^{13}C\{^1H\}$ NMR spectra of polypropylene produced at various propylene concentrations by **1d**/MAO.

Scheme 6
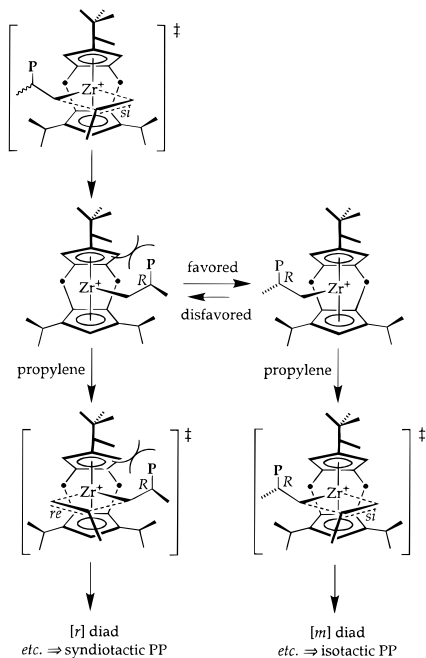
Figure 7. Methyl region of the $^{13}C\{^1H\}$ NMR spectra of polypropylene produced by **1d**,**e**/MAO and **2b**/MAO having [*r*] ≈ 50%

epimerization becomes competitive, allowing the chain a greater opportunity to migrate to the less hindered side of the metallocene wedge. In the limit of very low [propylene], the migratory insertion occurs preferentially from the same side of the metallocene wedge (with the same propylene enantioface, Scheme 6); isotactic polypropylene is produced. Apparently, **2b** operates with a different stereocontrol mechanism, since its stereoselectivity is essentially independent of propylene concentration (Figure 6), in agreement with the original proposals that its stereocontrol arises from regularly alternating insertions from stereospecific and aspecific sides of the metallocene wedge (without competitive site epimerization).[1d,4d,11]

At intermediate propylene concentrations, catalyst systems **1d**/MAO and **1e**/MAO produce a polypropylene with [*r*] = [*m*] ≈ 50% *that is not, however, atactic*. Rather, the pentad distributions (Figure 7) at [*r*] = 54% and [*r*] = 45% ([propylene] = 3.4 and 0.8 M, respectively) appear to be, at first glance, close to what is required for perfectly hemiisotactic polypropylene ([*mmmm*]:[*mmmr*]:[*rmmr*]:[*mmrr*]:[*mrmm*] + [*rmrr*]: [*mrmr*]:[*rrrr*]:[*rrrm*]:[*mrrm*] = 3:2:1:4:0:0:3:2:1). In fact, the $\{^1H\}^{13}C$ NMR spectra of the polymers produced by **1d**/MAO and **1e**/MAO under these conditions are quite similar to that produced by **2b**/MAO (Figure 7).

A closer examination of the microstructure of the hemiisotactic-like polypropylenes produced by **1d**/MAO and **1e**/MAO reveals some important differences from that of perfectly hemiisotactic examples: whereas the [*mrmr*] pentad is essentially absent (Figure 7, Table 7), that for [*mrmm*] + [*rmrr*], also strictly required to be missing for a perfectly hemiisotactic microstructure, is clearly present, comprising 9.1% and 9.4% of the pentads, respectively. For polypropylene generated by **2b**, these comprise only ca. 2%.[23,24] Further consideration of the consequences of the mechanism proposed in Scheme 6, in the limiting situation where the rate for the disfavored direction of site epimerization is zero, leads to the prediction that eight of the nine possible pentads should be observed, including [*rmrr*]. Only the [*mrmr*] pentad is predicted to be absent, as is

predominantly from regularly alternating sides of the metallocene wedge (and from alternating propylene enantiofaces, Scheme 6), and thus the system behaves syndiospecifically. However, as the propylene concentration is lowered, the second-order chain propagation process slows, and unimolecular site

(24) Since these pentads may arise from site epimerization, it may be the case that site epimerization does occasionally occur, even for **2b**/MAO.
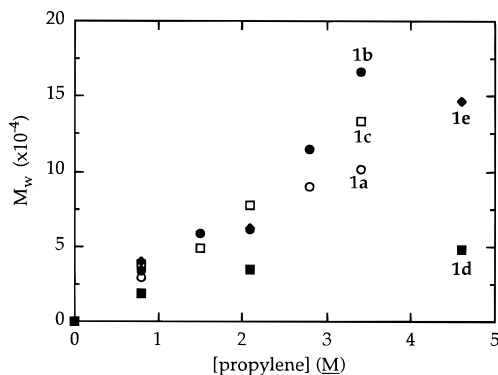
Figure 8. Dependence of molecular weights on propylene concentration for **1a**−**e**/MAO.

observed.[25] Thus, this model for stereocontrol does accommodate the observed polymerization behavior for C_1-symmetric catalyst systems *rac*-**1d**/MAO and enantiopure **1e**/MAO.[26]

Chain Transfer. Although there appears to be considerable scatter, the molecular weights (GPC) of the polymers produced by **1a**−**e**/MAO increase with increasing propylene concentration (Figure 8). A roughly linear increase with [propylene] is apparent for **1a**−**c**/MAO, suggesting that chain transfer is predominantly a unimolecular process.[27] On the other hand, catalysts **1d**,**e**/MAO display a less than first-order dependence of MW with [propylene], possibly indicating that chain transfer might depend on propylene concentration for these two systems. ^{1}H NMR analysis of low-molecular-weight polypropylene produced by **1d**/MAO at [propylene] = 0.5 M and 25 °C shows vinylidene signals at δ 4.72 and 4.80 ppm, indicative of chain transfer by β-H elimination. There are no signals attributable to vinylic end groups that would arise from β-CH$_3$ elimination. A primary kinetic isotope effect $k(\beta$-H)/$k(\beta$-D) of about 1.6 derived from the difference in number-average molecular weights of poly-d_0-propylene (32 800) vs poly-2-d_1-propylene (56 800) (vide supra), further suggests that chain transfer occurs primarily by β-H elimination. As is commonly found for α-olefin polymerization catalysts, a decrease in molecular weights with increasing temperature is also observed in liquid propylene and in toluene solution.[28]

(25) A full analysis of the possible pathways to the "allowed" pentads is given in the Supporting Information.

(26) The pentad distributions in the ^{13}C NMR spectra for polypropylenes produced by **1d**/MAO in neat propylene and in toluene solutions having differing [propylene] can be fit very well to a three-parameter model: one parameter (α) represents the monomer enantiofacial selectivity when the chain is on the less crowded side of the metallocene wedge, a second (β) represents (the same) monomer enantiofacial preference with the chain on the more crowded side of the metallocene wedge, and the third (ϵ) represents the probability of site epimerization wherein the chain moves from the less selective side to the more selective side (in the favored direction of Scheme 6). As required by the model in Scheme 6, least-squares fits give $\alpha \approx 0.99$, $\beta \approx 0.17$, and ϵ increases steadily as the [propylene] decreases from that in liquid propylene ($\epsilon \approx 0.12$) to 0.5 M ($\epsilon \approx 0.91$). Details of this statistical model will be presented in a forthcoming manuscript (Miller S. A.; Bercaw, J. E., manuscript in preparation).

(27) The dependence of the degree of polymerization (P_N) on propene concentration is a function of the rate of propagation (ν_P) vs rate of termination (ν_T) by β-H transfer to olefin (k_{TO}/k_P) or to metal (k_{TM}/k_P). Since PN = Mn/42 = ν_P/ν_T = C*k_P[C$_3$H$_6$]/C*(k_{TM} + k_{TO}[C$_3$H$_6$]), one obtains 1/PN = (k_{TM}/k_P)(1/[C$_3$H$_6$]) + k_{TO}/k_P. A plot of 1/PN vs 1/[propene] gives k_{TM}/k_P about 10^{-3} for **1a**−**e** and k_{TO}/k_P about 10^{-3} for **1d** and $\leq 10^{-4}$ for the other catalysts. These data suggest dominant monomolecular chain termination for **1a**−**c** and **1e** and partial contribution of a bimolecular process for **1d**. For analogous discussions, see: Stehling, U.; Diebold, J.; Kirsten, R.; Röll, W.; Brintzinger, H. H.; Jüngling, S.; Mülhaupt, R.; Langhauser, F. *Organometallics* **1994**, *13*, 964 and ref 8.

Conclusions

Some of the doubly silylene-bridged zirconocene catalysts investigated here have high syndiospecificity (>99.5%) for insertion of α-olefins into zirconium−polymeryl bonds. Loss of stereospecificity in these catalysts occurs mainly by stereochemical inversion at the metal center and, to a lesser extent, by a chain epimerization process which inverts the chirality of the β-carbon of the polymer chain. The R substituents (on the upper cyclopentadienyl ligand) of **1a**−**e** influence migratory olefin insertion and site and chain epimerization and transfer, and thus affect catalyst activity as well as the tacticity and molecular weight of the polypropylene. Although these effects are presently difficult to quantify, the polymerization data available suggest a significantly faster chain propagation for **1a** (R = H) than for the other catalysts, as shown by its astounding activity, while retaining relatively high syndiotacticity.

In comparison to Ewen/Razavi singly bridged fluorenyl/cyclopentadienyl zirconocene catalysts (e.g., **2a**/MAO) and aryl-substituted, singly bridged cyclopentadienyl/fluorenyl (e.g., **3**/MAO), the doubly [SiMe$_2$]-bridged catalysts described here display a slightly higher stereospecificity, but a stereoselectivity that appears to be more sensitive to changes in propylene concentration. A major difference in stereocontrol is observed for C_1-symmetric, doubly bridged **1d**,**e**/MAO as compared with singly bridged **2b**/MAO. The former catalyst systems, as a result of competitive chain propagation and site epimerization, produce polypropylenes of widely differing microstructures, from moderately syndiospecific through a form resembling hemiisotactic to moderately isotactic, as the propylene concentration decreases. The latter produces a polypropylene more closely matching hemiisotactic at all propylene concentrations examined, since site epimerization does not compete with propagation. These differences may be a result of the more open structures of the doubly [SiMe$_2$]-bridged zirconocene catalysts, permitting the polymer chain to swing more freely from side to side of the metallocene wedge.

Experimental Section

General Methods. All compounds were manipulated using high-vacuum line, Schlenk, cannula techniques or in a drybox under nitrogen atmosphere.[29] Argon and nitrogen gases were deoxygenated and dried by passage over columns of MnO on vermiculite and activated molecular sieves. Solvents were stored under vacuum over sodium benzophenone ketyl (THF, Et$_2$O, and (SiMe$_3$)$_2$O) or titanocene (toluene, petroleum ether) and freshly distilled immediately prior to use. Propylene was dried by passage through a Matheson 2110 drying system equipped with an OXISORB column. For polymerization experiments in toluene solutions, MAO (Albemarle) was used as a solid after removal of toluene in vacuo and being dried under high vacuum at 25 °C for 2 days. Comparisons of the activities between runs employing different MAO batches indicated strong deviations. ^{1}H, ^{2}H, and[13]C NMR spectra were recorded on a Bruker AM500 or a AMX500 at 500.13, 76.77, and 125.77 MHz, respectively. Elemental analyses were performed by Fenton Harvey of the Caltech Analytical Laboratory.

The compounds (Me$_2$C)[(η^5-C$_5$H$_3$Me)(η^5-C$_{13}$H$_8$)]ZrCl$_2$,[30] (Ph$_2$C)-[(η^{5-}C$_5$H$_4$)(η^{5-}C$_{13}$H$_8$)]ZrCl$_2$,[15a] metallocenes **1a**−**d**, and Me$_2$ClSi[C$_5$H$_3$-

(28) Propene polymerizations at [propene] = 3.4 M by **1b**/MAO produced a polymer of M$_w$ = 101 000 at 23 °C and 157 000 at 0 °C (PDI = 1.5 for both).

(29) Burger, B. J.; Bercaw, J. E. In *Experimental Organometallic Chemistry*; Wayda, A. L., Darensbourg, M. Y., Eds.; ACS Symposium Series 357; American Chemical Society: Washington, DC, 1987: Chapter 4.

(30) Razavi, A.; Atwood, J. L. *J. Organomet. Chem.* **1995**, *497*, 105.

3,5-(CHMe$_2$)$_2$][3a,31] were prepared as previously reported. (1*S*,2*S*,5*R*)-(+)-neomenthol was used as received (Aldrich), while (1*R*,2*S*,5*R*)-menthylcyclopentadiene was prepared by a slight modification of a recently reported preparation.[16] 6 2-*d*$_1$-Propylene was prepared as previously reported[9] and purified by distillation at −100 °C (cyclohexane/LN$_2$ slush) to a trap at −196 °C, passing through two traps at −80 °C. Gas chromatography and ^{1}H NMR analyses showed no traces of residual Et$_2$O. The product was stored at −80 °C in a Schlenk tube equipped with a Teflon valve. The concentration of propylene in toluene solutions was calculated according to literature data.[32]

Polymerization Reaction Procedures. The polymerization experiments in toluene solutions were carried out in a 250-mL glass reactor (Andrews Glass Co., maximum pressure 120 psi) equipped with a septum port, a large stir bar, and a pressure gauge (0−200 psi). *CAUTION: All of these procedures should be performed behind a blast shield.* Stirring was kept at 700 rpm. In a typical procedure, the glass reactor described previously was charged with solid MAO (180 mg for runs 1−5 and 500 mg for all others) and assembled in the drybox. The reactor was then connected to the propylene tank and purged with propylene at atmospheric pressure for 10 min. After this time, 40 mL of toluene was introduced in the reactor through the septum port. Under vigorous stirring, the reactor was purged again for an additional 15 min and, if necessary, pressurized for 10 min. The freshly prepared standard precatalyst solutions (1 mL) (0.42 mM, **1a**; 1.05 mM, **1b**; 0.98 mM, **1c**; 2.52 mM, **2b**, **1d**, and **1e**) were added by using a gastight syringe through the septum port. The polymerization reactions were quenched by slow addition of MeOH initially and then poured into 400 mL of HCl:MeOH (1:4) and stirred for about 4 h. Slow precipitation of the polymeric material from the toluene/MeOH solution allows an efficient elimination of aluminum residues from the polypropylene samples.

Bulk polymerization reactions were carried out in a 2-L steel reactor according to the following procedure. The reactor was purged with dinitrogen for several hours, 0.2 mL of a 10% MAO toluene solution was added, and condensed propylene was added. Under stirring (400 rpm), the temperature was then set at the desired value by use of an external metal jacket with circulating water. In the drybox, 4 mg of the metallocene was activated for 10 min with 9 mL of a 10% MAO toluene solution ([MAO]/[Zr] = 2000/1). An aliquot of this solution was then introduced into a 5-mL pressure chamber, which was then connected to the reactor and introduced into the reactor under N$_2$ pressure. The stirring was kept constant at about 400 rpm with a nitrogen flow controlled stirrer. After the given reaction time, the reactor was depressurized and the polymer collected and vacuum-dried overnight.

Polymerization of 2-*d*$_1$/*d*$_0$-Propylene. In a glovebox, a round-bottom flask was charged with 500 mg of solid MAO, assembled to a 90° needle valve, and the whole apparatus connected to a high-vacuum line. Toluene (50 mL) was vacuum transferred, and the whole assembly was saturated at atmospheric pressure with 2-*d*$_1$-propylene or *d*$_0$-propylene at 23 °C. The Teflon valve was then replaced by a septum, and 1 mL of a 2.52 mM standard toluene solution of **1b** was added by using a gastight syringe. After 10 min, the reaction mixture was quenched and the polymer treated as described above. This procedure was repeated 3 times for *d*$_0$-propylene and gave consistent productivities, which were comparable to the run with 2-*d*$_1$-propylene.

Polymer Analyses. Solution {^{1}H}^{13}C NMR spectra were recorded at 75.4 MHz on a Bruker AM500 or AMX500 spectrometer. Samples from the runs in toluene solution were prepared by mixing ca. 20 mg of the polymer in 0.6 mL of benzene-*d*$_6$:C$_6$H$_3$Cl$_3$:(SiMe$_3$)$_2$O (1:3:0.5), preheating at 80 °C for few hours, and measuring at that temperature. A total of 8000−10 000 transients were accumulated for each spectrum with a delay adjusted to have a recycling time of 4 s (12 s for poly-2-*d*$_1$-propylene). The samples for the experiments in neat propylene were prepared with ca. 5−7 mg of polymer in 0.6 mL of solvent. About 30 000 transients were acquired with 4 s recycling time. The chemical shifts are referenced to residual benzene-*d*$_6$ (128 ppm) or (SiMe$_3$)$_2$O (0 ppm). Decoupling was always on during acquisition, so NOE was

present. The polymer microstructures were obtained by analyzing the 18−22-ppm region in the {^{1}H}^{13}C NMR spectra, as previously described.[33]

Syntheses. C$_5$H$_5$-4-(1*R*,2*S*,5*R*-Menthyl) (4). To a solution of 5.0 g (32 mmol) of (1*S*,2*S*,5*R*)-(+)-neomenthol (degassed) in 150 mL of THF at −20 °C was added 20 mL (32 mmol) of a 1.6 M solution of *n*-BuLi in hexanes over 15 min. The temperature was kept constant for 1 h, and then a solution of 6.77 g (35 mmol) of tosyl chloride in 50 mL of THF was added over 20 min. The reaction mixture was allowed to warm to room temperature over 4 h and stirred for an additional 8 h. A solution of 3.52 g (32 mmol) of Na(C$_5$H$_5$) in 150 mL of THF was then slowly added to the reaction mixture at −10 °C under vigorous stirring over 30 min. After 2 h at −10 °C, the solution was warmed to room temperature and stirred for 14 h. The solution was then quenched with 15 mL of H$_2$O, the two phases were separated, and the water phase was extracted with 3 × 50 mL of Et$_2$O. The organic phases were collected, the solvent was removed in vacuo, and the product was Kugelrohr distilled at 70 °C/high vacuum, giving **4** in 72% yield (4.75 g, 23 mmol). The NMR analyses are consistent with the reported data.[16a]

Li[C$_5$H$_4$-4-(1*R*,2*S*,5*R*-menthyl)]. To a solution of 4.00 g (19.6 mmol) of **4** in 100 mL of Et$_2$O at 0 °C was added 12.5 mL (20 mmol) of a 1.6 M solution of *n*-BuLi in hexanes over 10 min. After the solution was stirred at −10 °C for 10 min, the cold bath was removed. Stirring was continued for 10 h at room temperature. The volume was then reduced to ca. 20 mL, and 100 mL of petroleum ether was vacuum transferred onto the reaction mixture. The product was filtered and dried overnight under vacuum, giving Li[C$_5$H$_4$-4-(1*R*,2*S*,5*R*-menthyl)] in 80% yield (3.3 g, 15.7 mmol). ^{1}H NMR (THF-*d*$_8$): δ 5.52−5.48 (m, 4H, Cp), 2.28 (m, 1H, Cp-C*H*), 1.62 (m, 1H, C*H* Me), 1.38 (m, 1H, C*H* Me$_2$), 1.26−0.80 (m, −CH$_2$−), 0.85 (d, $^3J_{HH}$ = 6 Hz, 3H, Me), 0.71 (d, $^3J_{HH}$ = 7 Hz, 3H, CH*Me$_2$*), 0.65 (d, $^3J_{HH}$ = 7 Hz, 3H, CH*Me$_2$*). ^{13}C NMR (THF-*d*$_8$): δ 125.1, 101.9, 101.6, 51.1, 48.7, 41.3, 36.8, 34.8, 27.8, 26.0, 25.6, 23.4, 22.2, 16.1.

(Me$_2$Si){C$_5$H$_4$-4-(1*R*,2*S*,5*R*-Menthyl)}{C$_5$H$_3$-3,5-(CHMe$_2$)$_2$} (5). To a solution of 2.30 g (9.5 mmol) of Me$_2$ClSi[C$_5$H$_3$-3,5-(CHMe$_2$)$_2$] in 100 mL of THF was added 2.00 g (9.52 mmol) of Li[C$_5$H$_4$-4-(1*R*,2*S*,5*R*-menthyl)] in 50 mL of THF at room temperature over 10 min. The resulting mixture was stirred overnight. Solvents were then removed in vacuo, and the residue was extracted with petroleum ether. Removal of the solvent gave **5** as a yellow oil in 92% yield (3.6 g, 8.7 mmol). ^{13}C NMR (benzene-*d*$_6$) (mixture of double bond isomers): δ 164.3, 161.3, 159.2, 157.0, 152.6, 152.3, 152.0, 150.7, 150.3, 150.1, 143.6, 143.4, 143.1, 142.9, 141.9, 134.3, 133.9, 133.7, 133.1, 132.4, 131.8, 131.3, 131.1, 130.8, 130.3, 127.4, 127.0, 126.8, 125.8, 125.1, 125.0, 124.6, 123.9, 123.8, 122.6, 122.3, 121.2, 52.2, 51.0, 50.9, 50.0, 49.3, 48.2, 48.0, 47.5, 47.2, 46.8, 46.3, 45.2, 45.0, 44.7, 44.5, 43.9, 42.9, 42.7, 42.3, 41.0, 40.2, 35.7, 35.6, 33.3, 33.1, 30.4, 30.2, 29.5, 28.2, 28.0, 25.3, 24.9, 24.8, 24.7, 23.8, 23.2, 22.8, 22.5, 22.2, 21.7, 21.1, 20.8, 15.7, 15.6, 2.0, 2.2, −3.9, −4.2, −4.7, −5.5. Elemental Anal. Calcd for C$_{28}$H$_{46}$Si: C, 81.95; H, 11.21. Found: C, 81.18, 81.33; H, 10.12, 10.42.

Li$_2$(Me$_2$Si){C$_5$H$_3$-4-(1*R*,2*S*,5*R*-Menthyl)}{C$_5$H$_2$-3,5-(CHMe$_2$)$_2$}. To a solution of 1.5 g (3.6 mmol) of **5** in 50 mL of Et$_2$O was added 5 mL (8 mmol) of a 1.6 M solution of *n*-BuLi in hexanes at room temperature over 5 min. The mixture was stirred for 24 h, and the solvent was removed in vacuo, leaving a white foam. Petroleum ether (3 × 20 mL) was vacuum transferred onto the reaction mixture and removed three times. The resulting powder was then washed with an additional 30 mL of petroleum ether and filtered, giving Li$_2$(Me$_2$Si){C$_5$H$_3$-4-(1*R*,2*S*,5*R*-menthyl)}{C$_5$H$_2$-3,5-(CHMe$_2$)$_2$} in 85% yield (1.3 g, 3.0 mmol). ^{1}H NMR (THF-*d*$_8$): δ 5.81, 5.78, 5.64, 5.62, 5.60 (s, 5H, Cp), 3.12 (m, 1H, C*H*Me$_2$), 2.75 (m, 1H, C*H*Me$_2$), 2.31 (m, 1H, −CH−), 1.61 (m, 1H, −CH−), 1.37 (m, 1H, C*H*Me$_2$), 1.26−1.03 (m, −CH$_2$−), 1.13 (d, $^3J_{HH}$ = 6 Hz, 6H, CH*Me$_2$*), 0.85 (d, $^3J_{HH}$ = 6 Hz, 3H, Me), 0.71 (d, $^3J_{HH}$ = 6 Hz, 3H, CH*Me$_2$*), 0.65 (d, $^3J_{HH}$ = 6 Hz, 3H, CH*Me$_2$*), 0.26 (s, 6H, SiMe), 0.25 (s, 6H, SiMe). ^{13}C NMR (THF-*d*$_8$): δ 134.8, 128.1, 127.7, 122.1, 118.8, 110.5 (broad), 108.2, 107.2, 104.1 (broad), 101.9, 101.6, 100.5, 98.7, 94.2, 51.1, 50.8, 48.8, 43.5, 36.8, 34.7, 30.5,

(31) Yoder, J. C.; Day, M. W.; Bercaw, J. E. *Organometallics* **1998**, *17*, 4946.

(32) Frank, H. P. *Öster. Chem. Zeit.* **1967**, *11*, 360.

(33) Busico, V.; Cipullo, R.; Corradini, P.; Landriani, L.; Vacatello, M.; Segre, A. L. *Macromolecules* **1995**, *28*, 1887.

30.2, 29.7, 27.8, 27.3, 26.1, 25.9, 25.6, 25.4, 25.3, 25.1, 24.9, 23.4, 22.3, 22.2, 19.2, 16.1, 14.2, 3.1 (Si*Me*$_2$). Elemental Anal. Calcd for C$_{28}$H$_{44}$Si$_2$Li$_2$: C, 79.64; H, 10.42. Found: C, 77.32, 77.30; H, 11.50, 11.44.

(1,2-Me$_2$Si)$_2${C$_5$H$_3$-4-(1*R*,2*S*,5*R*-Menthyl)}{C$_5$H$_2$-3,5-(CHMe$_2$)$_2$} (6). To a solution of 1.93 g (4.6 mmol) of Li$_2$(Me$_2$Si){C$_5$H$_3$-4-(1*R*,2*S*,5*R*-menthyl)}{C$_5$H$_2$-3,5-(CHMe$_2$)$_2$} in 50 mL of THF at −78 °C was vacuum transferred 1.0 g (1.1 mL, 5 mmol) of SiMe$_2$Cl$_2$. The resulting mixture was stirred at that temperature for 4 h and then warmed to room temperature over 4 h. After the solution was stirred for an additional 20 h at room temperature, the volatiles were removed, and the product was extracted with 100 mL of petroleum ether. Removal of the solvent gave a yellow oil, which was then Kugelrohr distilled twice at 120 °C/high vacuum. White solid **6** was obtained in 83% yield (1.8 g, 3.8 mmol). ^{13}C NMR (benzene-*d*$_6$): δ 162.7, 162.2, 151.3, 151.1, 146.5, 146.3, 140.2, 139.4, 138.9, 132.3, 131.9, 131.8, 131.4, 131.1, 130.9, 130.7, 123.3, 123.2, 56.8, 56.6, 47.5, 47.3, 45.6, 45.3, 42.8, 35.7, 33.4, 30.0, 29.9, 29.5, 27.9, 27.8, 24.9, 24.8, 23.2, 22.9, 22.0, 15.3, 0.6, 0.5, −3.2, −6.2. Elemental Anal. Calcd for C$_{30}$H$_{49}$Si$_2$: C, 77.24; H, 10.72. Found: C, 76.93; H, 10.98.

[(1,2-Me$_2$Si)$_2${η^5-C$_5$H$_2$-4-(1*R*,2*S*,5*R*-Menthyl)}{η^5-C$_5$H-3,5-(CHMe$_2$)$_2$}]ZrCl$_2$ (1e). To a solution of 600 mg (1.3 mmol) of **6** in 50 mL of Et$_2$O at room temperature was added 1.8 mL (2.85 mmol) of a 1.6 M solution of *n*-BuLi in hexanes. After the solution was stirred at 25 °C for 20 h, a suspension of 350 mg (1.5 mmol) of ZrCl$_4$ in 20 mL of Et$_2$O was added via cannula to the solution of Li$_2$[(1,2-Me$_2$-Si)$_2${η^5-C$_5$H$_2$-4-(1*R*,2*S*,5*R*-menthyl)}{η^5-C$_5$H-3,5-(CHMe$_2$)$_2$}] (**7**), and the reaction mixture was stirred for 22 h. The resulting precipitate was filtered, and the filtrate was dried in vacuo. The resulting powder was then washed with cold hexamethyldisiloxane. Yield: 290 mg (46%). ^{1}H NMR (benzene-*d*$_6$): δ 6.80 (s, 1H, Cp), 6.73 (s, 1H, Cp), 6.46 (s, 1H, Cp), 2.92−2.99 (m, 2H, Cp-C*H*Me$_2$), 2.75−2.82 (m, 2H, −CH−), 1.79−1.52 (m, 4H, −CH$_2$−), 1.36 (d, $^3J_{HH}$ = 6 Hz, 3H, C*H*Me$_2$), 1.21 (m, 2H, −CH$_2$−), 1.01 (d, $^3J_{HH}$ = 7 Hz, 3H, CH*Me*$_2$), 0.96 (d, $^3J_{HH}$ = 7 Hz, 3H, CH*Me*$_2$), 0.95 (d, $^3J_{HH}$ = 7 Hz, 3H, CH*Me*$_2$), 0.76 (d, $^3J_{HH}$ = 7 Hz, 3H, CH*Me*$_2$), 0.73 (d, $^3J_{HH}$ = 7 Hz, 3H, CH*Me*$_2$), 0.57, 0.53, 0.50, 0.48 (s, 3H, Si*Me*$_2$). ^{13}C NMR (C$_6$D$_6$): δ 3.0 (SiMe$_2$), 3.3 (SiMe$_2$), 15.6, 20.5, 20.6, 21.7, 22.7, 24.9, 27.9, 28.3, 28.2, 29.2, 29.3, 33.3, 35.4, 41.3, 43.4, 50.6, 108.3, 108.5, 113.6, 114.8, 133.63, 138.5, 139.0, 163.8, 166.2. Elemental Anal. Calcd for C$_{30}$H$_{47}$Cl$_2$Si$_2$Zr: C, 57.59; H, 7.51. Found: C, 56.38, 56.19; H, 7.73, 7.60. Li$_2$[(1,2-Me$_2$Si)$_2${η^5-C$_5$H$_2$-4-(1*R*,2*S*,5*R*-menthyl)}{η^5-C$_5$H-3,5-(CHMe$_2$)$_2$}] (**7**) can be obtained as a THF adduct in crystalline form by cooling at −30 °C a concentrated Et$_2$O/petroleum ether solution containing a few drops of THF.

Supporting Information Available: Schemes detailing the possible pathways to the "allowed" pentads with catalyst **1d**/MAO. Details of the structure determinations, including listing of final atomic coordinates, thermal parameters and bond distances and angles (56 pages, print/PDF). See any current masthead page for ordering information and Web access instructions.

JA982868J